LOW FREQUENCY FLEXTENSIONAL TRANSDUCER DESIGNS FOR OCEAN ACOUSTIC TOMOGRAPHY

J. Ahmad, D.T.I.Francis & R.F.W.Coates

School of Electronic and Electrical Engineering, University of Birmingham, Birmingham, U.K.

1. INTRODUCTION

Ocean Acoustic Tomography, a process similar to medical tomography which uses X-rays to map the density variations and hence internal organs of the body, is a technique whereby the physical characteristics of a region of the ocean can be measured by acoustic means. This can be achieved by the deployment of acoustic transducers around the periphery of an ocean basin so that they transmit pulse-like signals to receivers separated by several hundred kilometres. Changes in the times of flight of the acoustic emanations can then be used to determine physical factors of interest encompassing temperature fluctuations, sound speed profiles, density variations and velocity distributions. Observation of a wide sea area requires the use of low frequency (LF) sound to enable transmission distances of several hundred kilometres. Unfortunately, LF transducers tend to be large, heavy and expensive. This paper investigates the development of a compact, concave LF (400 Hz) flextensional transducer design able to project high acoustic power efficiently over a broad frequency range. The design and modelling work is performed by three dimensional Finite Element/Boundary Element numerical methods by varying important design parameters and observing their effects on the performance of the device. Designs are presented which meet the specified objectives and predicted performance characteristics are reported.

2. TRANSDUCER DESIGN AND MODELLING TECHNIQUES

The many methods of transducer design in existence include techniques such as the Finite Element method, the method of Finite Differences and equivalent circuit techniques. The FE method entails numerically solving partial differential equations which have been derived by dividing the structure into elements, defining nodal positions and then applying shape functions, normally polynomials, to approximate the variables. The method of Finite Differences entails replacing all derivatives in the equation by finite difference expressions, for example, by using Taylor series expansions, thus resulting in a discrete set of algebraic equations which can be solved in matrix form. However, this method is not very accurate. Finally, equivalent circuit techniques involve the use of standard electro-mechanical analogies to model the mechanical attributes of the device. This is achieved by applying conventional circuit analysis techniques to equivalent electrical networks. Unfortunately, equivalent circuit techniques over-simplify the mechanical design and only allow treatment in one dimension.

The Finite Element Method is now widely used in the analysis of piezoelectric transducers and is the commonest solution to the problem of simulating broadband and mechanically complex structures. Modelling work in this paper has been performed using the Finite Element method as it allows for the modelling of much more complicated devices than is possible with other numerical methods. The Finite Element method has been discussed at length in the ample literature available on the subject, for example references [1], [2] and so will not be reviewed here.

3. DESIGN AND MODELLING OF THE CLASS III "WAISTED" FLEXTENSIONAL TRANSDUCER

Finite Element calculations were performed to establish the influence of design parameters on the performance characteristics of the flextensional transducer. Transducer performance trends due to varying aluminium stave thickness (t), curvature of the shell profile ($c=1/r$), total number of staves in the device (n), end plate radius (r_e) and thickness (h_e), size ratio (s) and ceramic cross sectional area (A) have been examined, these parameters being illustrated in the section view of Figure 1 and their base values listed in Table 1. r_c and R_c are the inner and outer radii of the ceramic stack and l is the length of the device between the end plates. It should be noted that r_e is the radial distance from the axis to the mid-point of one of the sides, and includes the thickness of the stave. An aluminium shell is used throughout due to its superior performance as was observed in preliminary analyses [3]. Figure 2 illustrates the complete surface of the FE model. Rotational symmetry is exploited in the design process so that only one segment is subject to analysis.

The performance parameters considered are those which are most relevant to the application - frequency (*f*), power output (*w*) and bandwidth (Q factor). The aim is to achieve low frequency (400 Hz) with good power output (190 dB ref. 1 μPa at 1 metre) and a Q factor close to 4, in as compact a device as possible.

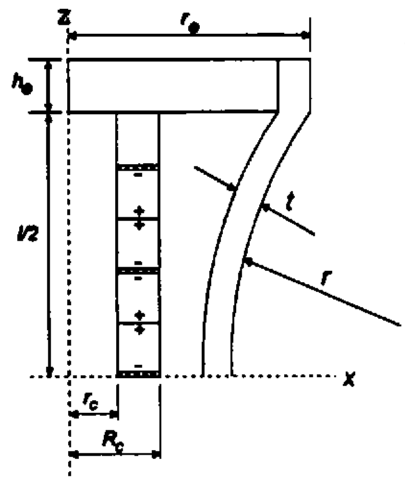

Figure 1: Parameters in Transducer Shell Design

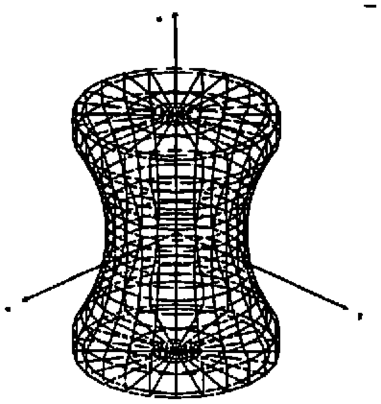

Figure 2: Flextensional Class III Transducer Shell

Table 1: Design Parameters and their Base Values

Parameter	Base Value
r	0.3m
$c=1/r$	$3.33m^{-1}$
t	0.015m
$l/2$	0.125
r_e	0.085
h_e	0.03
r_c	0.02
R_c	0.04
$A=\pi(R_c^2-r_c^2)$	$3770mm^2$
n	24
s	(1)

4. RESULTS AND ANALYSIS

Stave Thickness

Predicted performance parameters corresponding to variations in the stave thickness were presented in [3]. Recapitulating, the fundamental resonant frequency was observed to increase linearly as the staves became thicker and thus more stiff. The power generated from the device reached a peak for an 8mm shell, thicker shells producing less and less power. The Q factor, which is the ratio of resonant frequency to 3dB bandwidth as determined from the conductance response, was seen to decrease with increasing shell thickness which may be attributed to an increased shell coupling, i.e. the thicker shells were able to radiate the energy developed in the ceramic more effectively. This would suggest further decreases in the Q factor should the device staves become even thicker. However, for the primary design dimensions it was impossible to increase the shell thickness any further for a fixed end plate area as thicker shells produced a shell-stack overlap constituting an impractical configuration.

Stave Curvature

Transducer performance was observed as the radius of shell profile was varied from r=25cm (very concave) to r=80cm (almost straight) for models with 8mm thick and 15mm thick shells. The performance curves obtained from the *in-water* models were listed in [3]. The characteristics showed the predicted resonant frequency to decrease with increasing radii of curvature and thus straighter-staved devices. In addition, the device was observed to generate less power at a higher Q factor as the staves becomes straighter. This may be attributed to the greater difficulty associated with exciting the flexural mode in the straighter staved devices and suggests that although the flextensional concept involves amplifying the stack motion, attempting to achieve excessive amplification can be counter-productive. The results would therefore suggest that a stave with small radius of curvature be used in the final design. r=30cm would seem to be a reasonable choice for the given length since r=25cm corresponds to a hypothetical model in which the staves overlapped the ceramic stack.

Number of Staves

The effect of varying the number of staves while keeping the radiating area of the staves constant is illustrated in Figure 3, where the results for an aluminium-staved device (n=4 to n=24) with a fixed radius of curvature of 30cm, are presented for two stave thicknesses of 8mm and 15mm.

Increasing the total number of staves has the effect of increasing the frequency, reaching a plateau at about 10 staves. Similarly, the power output and Q factor decrease down to about 10 staves, and then level off. These trends suggest that the number of staves in the flextensional device is not really of paramount importance unless very few staves are incorporated in the structure. A device consisting of 12 radiating staves would appear a reasonable choice as such a device would not present too much demand during construction and this number has been chosen for the purposes of the subsequent analyses.

Size Ratio

A 12-staved aluminium-shelled device with r=30cm and original thickness t=15mm is scaled by applying a constant scale factor to all linear dimensions. Results obtained from FE/BE calculations performed on these devices are shown in Figure 4.

As expected, the larger transducers resonate at lower frequencies, the frequency being inversely proportional to the size of the device. Predictably, as a consequence of an increased radiating area, the bigger devices also generate more power, the increase following a square law. No change is observed in the Q factors since effectively the same device, equally scaled in all linear dimensions, is being modelled, thus producing similar conductance responses. These results correspond to the theoretical relationships,

$$f \propto 1/s \tag{1a}$$

$$w \propto s^2 \tag{1b}$$

$$Q = \text{constant} \tag{1c}$$

derived in [4].

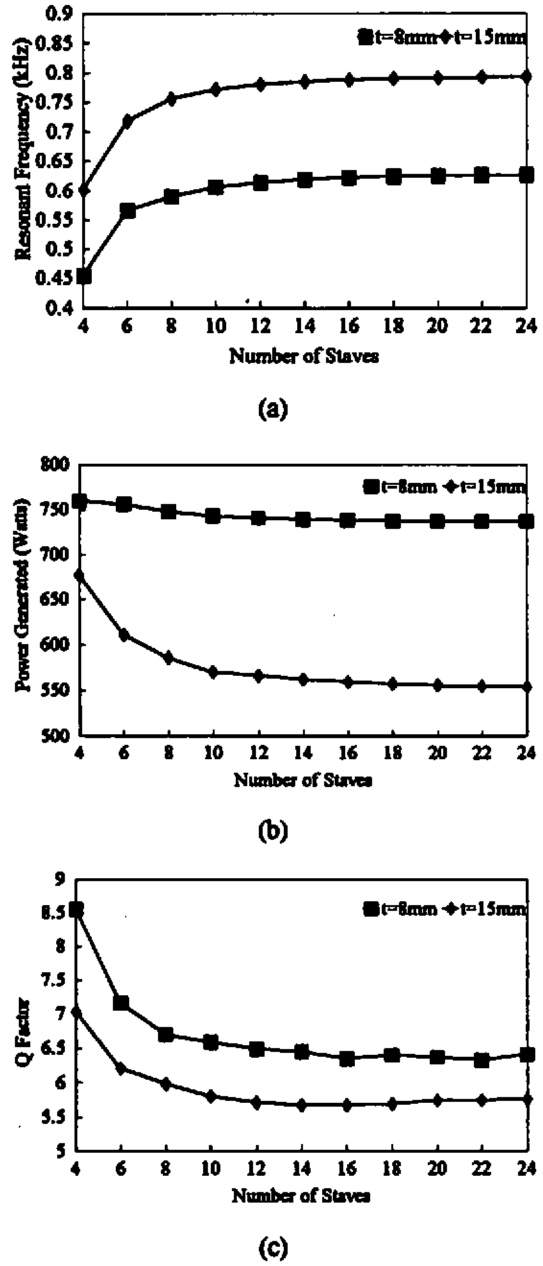

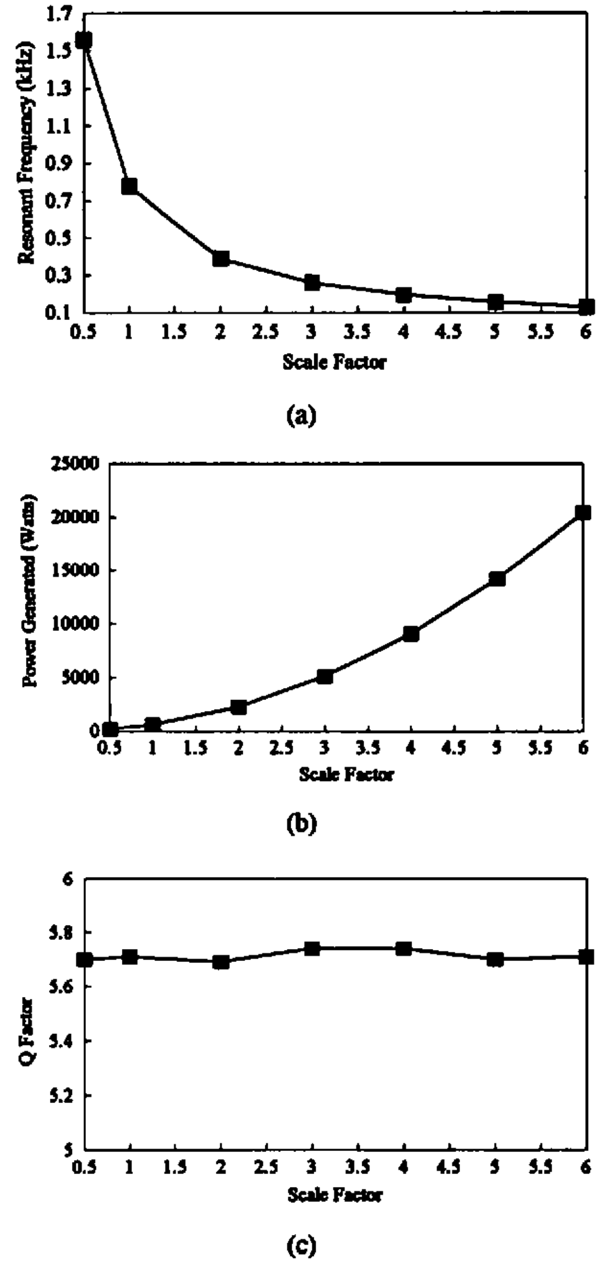

Figure 3: Effect of varying the Number of Staves on the Transducer Performance Parameters (a) Fundamental Resonance (kHz), (b) Power Generated (Watts), (c) Q Factor

Figure 4: Effect of varying the Size of the Device on the Transducer Performance Parameters (a) Fundamental Resonance (kHz), (b) Power Generated (Watts), (c) Q Factor

End Plate Parameters

The function of the transducer end plate is to transfer energy from the ceramic to the staves which are responsible for radiating the energy into the water. The characteristics of the end plate are therefore important. The effect of varying the properties and dimensions of the end plates on the performance characteristics of the flextensional device are observed in this section.

A. Varying End Plate Radius for different End Plate Materials

In order to examine what effect the end plate stiffness has on the device performance, a 12 staved transducer with r=30cm and t=15mm is simulated in water for end plates of aluminium, steel and super stiff steel (a hypothetical material with a stiffness 10 times that of steel) and stycast. The super stiff material is modelled to reduce the effect of flexing in the end plate so as to isolate the dependence on the shell more effectively. The end plate radius, r, is scaled from its base value of 0.085m. The FE predicted performance characteristics are shown in Figure 5.

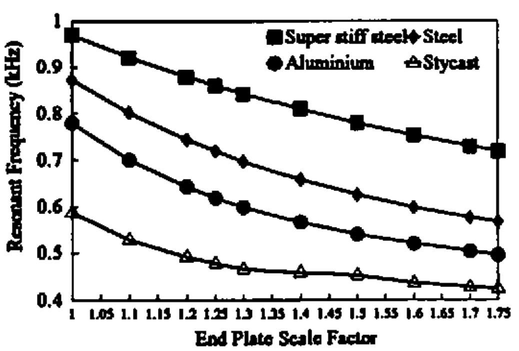

(a)

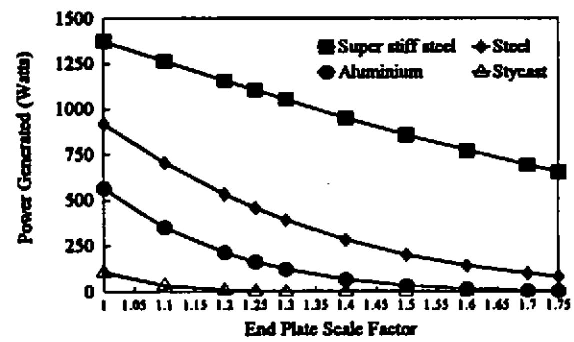

(b)

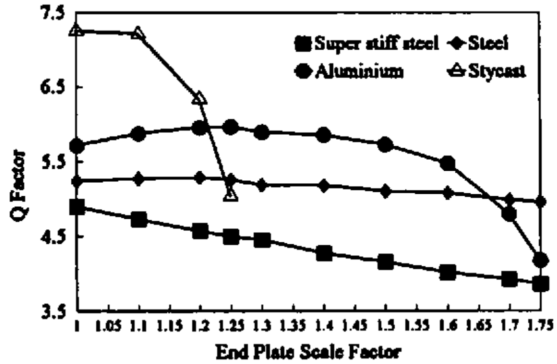

(c)

Figure 5: Effect of varying the End Plate Radius on the Transducer Performance Parameters (a) Resonant Frequency (kHz), (b) Power Generated (Watts), (c) Q Factor, for different End Plate Materials

These results show that as the end plate gets wider, the increased mass causes the device to resonate at reduced frequencies regardless of the material composition. The stiffer end plates contribute towards stiffer overall structures which resonate at the higher frequencies.

Various factors contribute to the effect on the acoustic power. An increased radius increases the radiating area and may therefore be expected to increase the power. However, this appears to be outweighed by two other factors. Firstly, as the radius increases, the end plate becomes more flexible and therefore less effective in transferring power to the staves thus resulting in a reduced power generated from the device. In addition, lowering the resonant frequency results in a reduction in radiated power because of the reduced volume displacement per unit time for a given displacement amplitude of the radiating surface. For similar reasons, the stiffer materials produce greater acoustic powers and show less deterioration with increasing radius. Stycast, which is relatively compliant, would be a bad choice for the end plate material as it is far too flexible to transfer energy efficiently to the shell.

The Q factor does not appear to be very much affected by changes in the end plate radius, except for the case of stycast in which it reduces quite rapidly; this can be attributed in part to mechanical losses in the material itself. Q factor results for an end plate with a radius scale factor greater than 1.25 are not determinable for this material due to extremely low conductance peaks not even detected by the FE model. This is probably due to the end plates becoming far too flexible to transfer energy efficiently to the shell. The stiffer end plates produce the lower Q values albeit at higher resonant frequencies. These results suggest that a stiff end plate such as steel, with a relatively small end plate radius be used in the final device as it offers good energy transfer characteristics. Work completed in the remaining section is therefore based on a model with a steel end plate.

B. Varying End Plate Thickness with respect to the End Plate Radius

The effect of varying the thickness of steel end plates is investigated in this section for varying end plate radius. A small sample of end plate radii r_e={0.085, 0.09, 0.095, 0.1, 0.11, 0.12}m is investigated for various end plate thicknesses h_e={0.02, 0.03, 0.04, 0.05, 0.06}m for a fixed 15mm thick aluminium shell. Figure 6 presents the simulation results in three dimensions so that global trends can be observed.

In Figure 6(a), the structure is seen to resonate at a higher frequency as the thickness and hence stiffness of the end plate increases, the wider end plates boasting the lower resonances. The lowest resonant frequencies occur for the wide and thin (flexible) end plates. Again, the thicker and thus stiffer end plates are able to transfer energy more efficiently to the shell and therefore produce greater powers and lower Q factors, as observed in Figures 6(b) and 6(c), the wider end plates producing lower powers and generally lower Q factors. The greatest powers are generated from structures with narrow end plates, whereas the lowest Q factors are produced by those devices with thick, wide end plates.

The conclusions drawn from these results suggest that a sufficiently thick (for example, h_e=0.04 or 0.05) end plate with a reasonable radius (for example, r_e=0.1) be chosen in the final device design in order to optimise the performance parameters, in particular the Q factor as much as possible at this stage. This will ensure that the end plate does not become too flexible resulting in insufficient power output or too thick and heavy.

C. Varying End Plate Thickness with respect to the Stave Thickness

The effect of varying the stave thickness for models with different end plate thicknesses are now observed. This time a longer end plate radius of r_e=0.1 allows for thicker (15-30mm) staves to be incorporated into the design. Calculated performance characteristics are shown in Figure 7. The trends observed are as expected from previous results. The lowest resonant frequency occurs for device designs with thinnest stave and end plate thicknesses and increases as t or h_e increase. Greatest power output is observed for thick end plate devices with thin staves and deteriorates as the staves become thicker or the end plates thinner. Finally, best Q factor results are obtained for thick shelled, thick end plate devices.

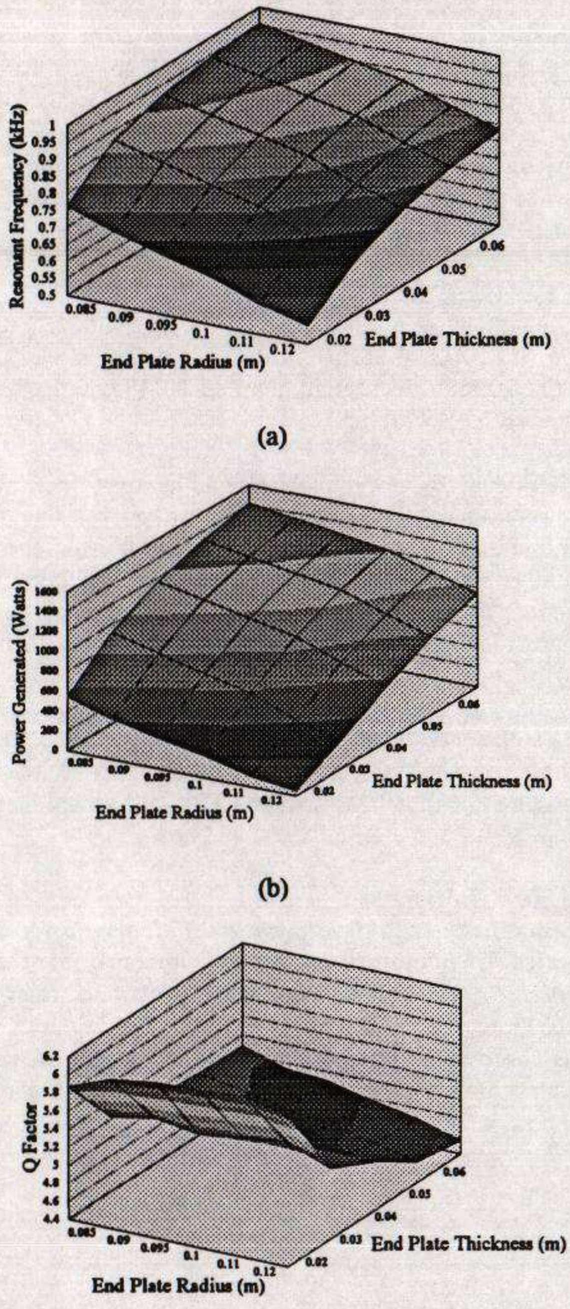

Figure 6: Effect of varying End Plate Thickness for different End Plate Radii, on (a) Fundamental Resonant Frequency, (b) Power Output and (c) Q Factor

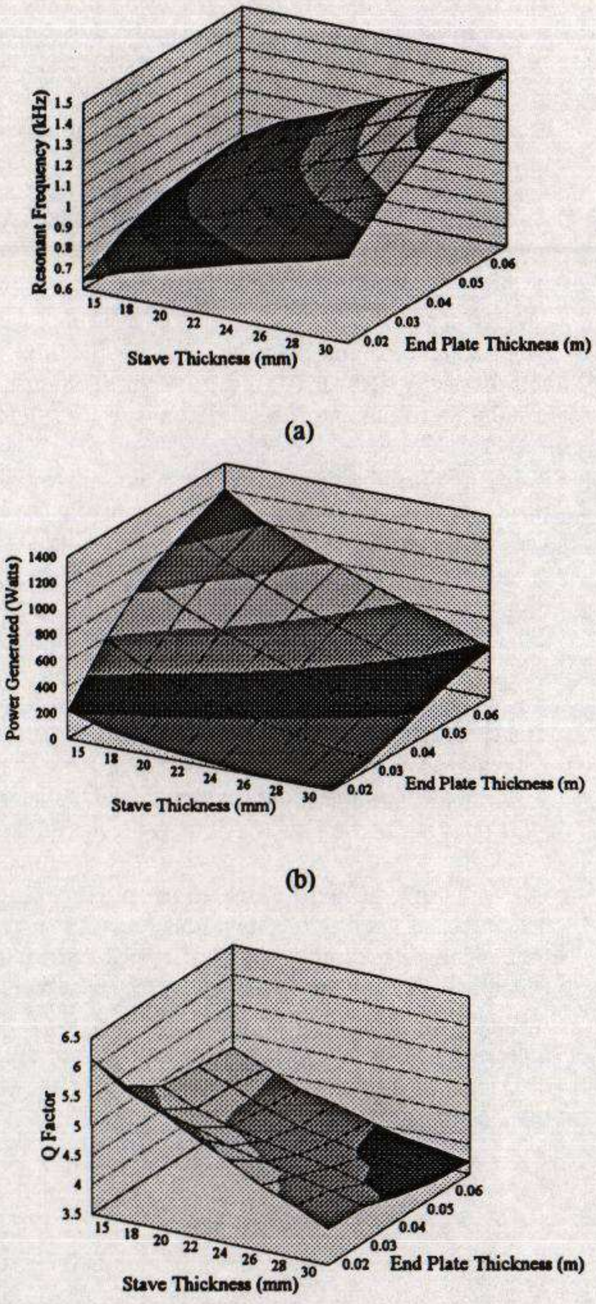

Figure 7: Effect of varying End Plate Thickness for different Stave Thicknesses, on (a) Fundamental Resonant Frequency, (b) Power Output and (c) Q Factor

Further Variation in the Stave Curvature

The larger end plate radius r_e=0.1 allows for smaller stave curvatures to be used in the design. Results for r={15,20,25,30,40,50,60}cm and h_e=0.04 and stave thicknesses of 15mm and 20mm are shown in Figure 8.

The performance characteristics show that a device with a smaller than maximum possible stave t for r_e=0.1 with a smaller stave radius of curvature (<30cm) is not as beneficial as a device with larger t and a larger value of r as the former produces larger Q values and large fundamental resonant frequencies.

Varying Ceramic Area

The cross sectional area A of the central ceramic stack is changed by applying a radial scale factor to the ceramic discs. The results presented in Figure 9 are for a device with r=30cm, h_e=0.04 and r_e=20mm as the A is varied.

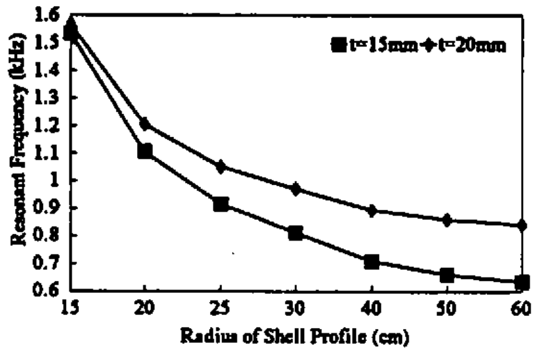

(a)

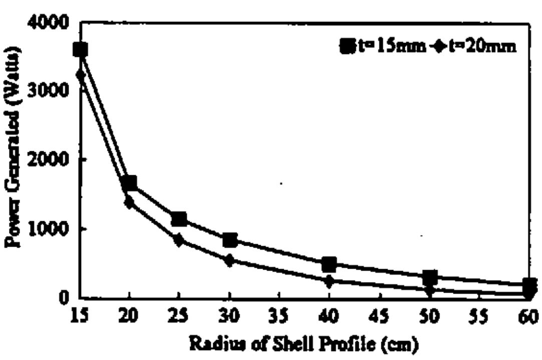

(b)

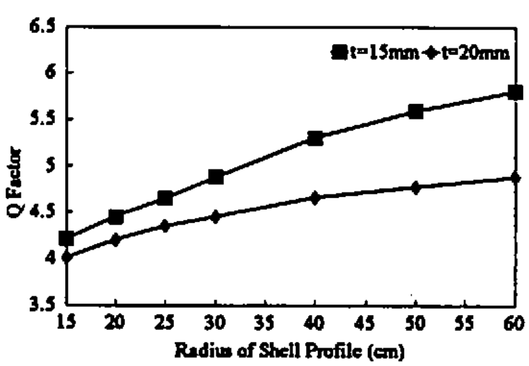

(c)

Figure 8: Variation of Transducer Performance Parameters (a) Resonant Frequency (kHz), (b) Power Generated (Watts), (c) Q Factor, with Radius of Shell Profile

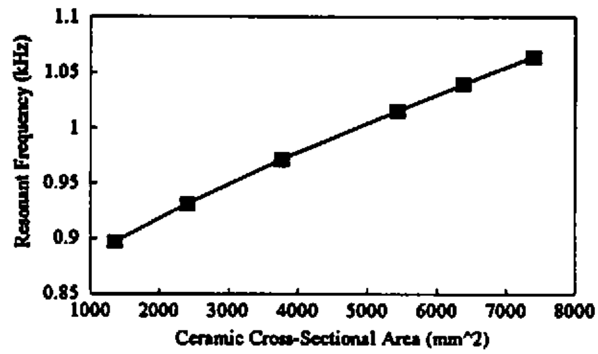

(a)

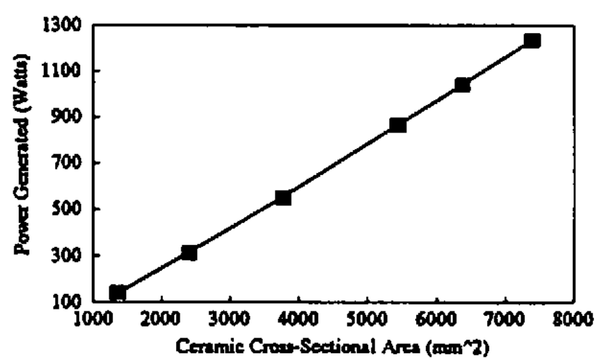

(b)

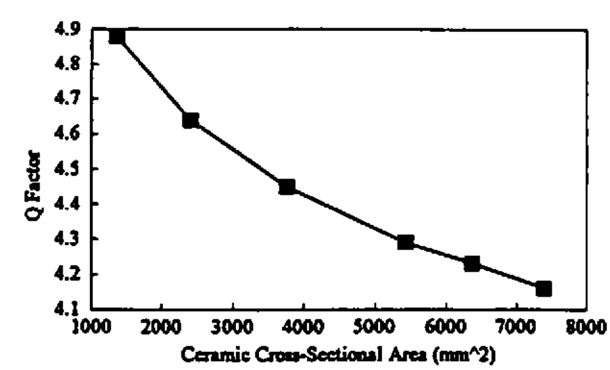

(c)

Figure 9: Effect of varying the Ceramic Cross-Sectional Area on the Transducer Performance Parameters (a) Resonant Frequency (kHz), (b) Power Generated (Watts), (c) Q Factor

The resonant frequency of the stack-shell combination increases with increasing ceramic cross sectional area due to the increased stiffening of the structure. This change in frequency is not very significant as a five fold increase in A produces only a 20% increase in frequency. The acoustic power radiated increases with increasing A because the increased volume of ceramic transfers more energy to the end plates which results in increased stave vibration and hence greater radiation of acoustic power. An approximate relationship $w \propto Af^2$ exists. That is, more power than would be expected from a simple relationship $w \propto A$ is generated. This increase at a factor greater than just the area may be attributed to the increasing stave frequency with A which results in higher stave velocity and thus more power output. The increase in overall Q factor with A may be attributed to (a) the end plate influence; for a small ceramic A, the end plate has a greater compliance which decouples the staves from the stack and thus the greater ceramic A configurations provide better coupling and therefore lower Q values, (b) resonant frequency effects; for greater A, a higher resonance frequency has the effect of increasing the loading on the transducer staves hence producing a lower Q factor.

5. OPTIMUM DESIGN OPTIONS

The results presented in this paper can be collated to produce a number of possible design options, three of which are listed here. In each case, the basic device design parameters are scaled appropriately, according to the conclusions drawn from varying *size ratio* predictions, to achieve resonance at 400Hz.

DESIGN OPTION (1)

Basic Device Design		Scaled Device Design (s=3.1425)	
Parameter Values	Performance Characteristics	Parameter Values	Performance Characteristics
r=0.30 m	f=1.257kHz	r=0.94 m	f=400Hz
t=0.028 m	w=244.25 W	t=0.088 m	w=2.41 kW
l=0.25 m	Q=4.0	l=0.79 m	Q=4.0
r_e=0.10 m		r_e=0.31 m	
h_e=0.04 m		h_e=0.13 m	
r_c=0.02 m		r_c=0.06 m	
R_c=0.04 m		R_c=0.13 m	
n=12		n=12	

DESIGN OPTION (2)

Basic Device Design		Scaled Device Design (s=3.015)	
Parameter Values	Performance Characteristics	Parameter Values	Performance Characteristics
r=0.20 m	f=1.206kHz	r=0.603 m	f=400Hz
t=0.020 m	w=1.396 kW	t=0.060 m	w=12.69 kW
l=0.25 m	Q=4.2	l=0.75 m	Q=4.2
r_e=0.10 m		r_e=0.30 m	
h_e=0.04 m		h_e=0.12 m	
r_c=0.02 m		r_c=0.06 m	
R_c=0.04 m		R_c=0.12 m	
n=12		n=12	

DESIGN OPTION (3)

Basic Device Design		Scaled Device Design (s=2.5975)	
Parameter Values	Performance Characteristics	Parameter Values	Performance Characteristics
r=0.30	f=1.039 kHz	r=0.78 m	f=400 Hz
t=0.02	w=1.043 kW	t=0.052 m	w=7.04 kW
l=0.25	Q=4.2	l=0.65 m	Q=4.2
r_e=0.10		r_e=0.26 m	
h_e=0.04		h_e=0.10 m	
r_c=0.026		r_c=0.07 m	
R_c=0.052		R_c=0.14 m	
n=12		n=12	

The lowest Q factor is obtained by the first design option. However, if a slight sacrifice is allowed for in the Q factor, as in the latter two designs, then a more compact device can be used. In design (2), a smaller r and t are used to achieve compactness, whereas in design (3), a greater ceramic area enables the device to be more compact.

6. CONCLUSIONS

Transducer design options have been presented for a high power, low Q Class III concave-staved flextensional transducer resonating at 400 Hz suited to ocean acoustic tomography. The steps leading up to the optimisations have been presented and performance characteristics displaying the trends shown.

7. ACKNOWLEDGEMENTS

This research was performed for the European Community, Marine Science and Technology (MAST) Directorate under the LOFTOMO Contract MAS2-C291-0010-C.

8. REFERENCES

[1] Hardie, D.J.W., "Introduction to Finite Elements", *Proc. Inst. Acoust.*, vol. 10(9), pp. 1-15, 1988.

[2] Smith, B.V., "Finite Element Principles", *Proc. Inst. Acoust.*, vol. 10(9), pp. 16-37, 1988.

[3] Francis, D.T.I., Ahmad, J., Bayliss, C. & Coates, R.F.W., "Finite and Boundary Element Modelling of Class III Flextensional Transducers for Ocean Acoustic Tomography", *Proc. Second European Conference on Underwater Acoustics*, vol. I, pp. 515-520, 1994.

[4] Francis, D.T.I., Bayliss, C., Ahmad, J. & Coates, R.F.W., "The Development of a Low Frequency Barrel-Stave Transducer for Tomographic Applications using Finite Element and Boundary Element Modelling", *IEEE Proc. Oceans 94*, vol. I, pp. 371-376, 1994.